CrossMark
click for updates

View Article Online
View Journal

Molecular BioSystems

Accepted Manuscript

This article can be cited before page numbers have been issued, to do this please use: F. Lopez-Moya, D. Kowbel, M. J. Nueda, J. Palma-Guerrero, N. L. Glass and L. V. Lopez-Llorca, *Mol. BioSyst.*, 2015, DOI: 10.1039/C5MB00649J.

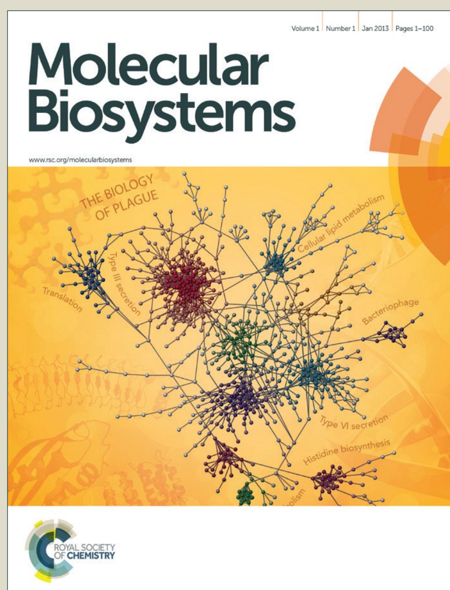

This is an *Accepted Manuscript*, which has been through the Royal Society of Chemistry peer review process and has been accepted for publication.

Accepted Manuscripts are published online shortly after acceptance, before technical editing, formatting and proof reading. Using this free service, authors can make their results available to the community, in citable form, before we publish the edited article. We will replace this *Accepted Manuscript* with the edited and formatted *Advance Article* as soon as it is available.

You can find more information about *Accepted Manuscripts* in the Information for Authors.

Please note that technical editing may introduce minor changes to the text and/or graphics, which may alter content. The journal's standard Terms & Conditions and the Ethical guidelines still apply. In no event shall the Royal Society of Chemistry be held responsible for any errors or omissions in this *Accepted Manuscript* or any consequences arising from the use of any information it contains.

ROYAL SOCIETY OF CHEMISTRY

www.rsc.org/molecularbiosystems

View Article Online
DOI: 10.1039/C5MB00649J

Published on 01 December 2015. Downloaded by Universidad de Alicante on 09/12/2015 15:48:54.

Novelty of the work

In this work we performed the first transcriptional study of a filamentous fungus (*N. crassa*) in response to chitosan.

Graphic

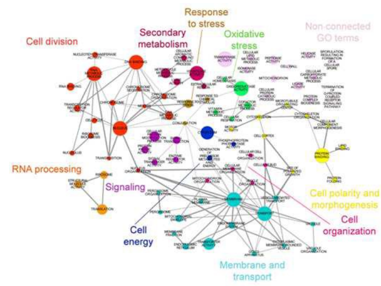

Molecular BioSystems Accepted Manuscript

View Article Online
DOI: 10.1039/C5MB00649J

Published on 01 December 2015. Downloaded by Universidad de Alicante on 09/12/2015 15:48:54.

1 ***Neurospora crassa* transcriptomics reveals oxidative stress and plasma membrane**
2 **homeostasis biology genes as key targets in response to chitosan**

3 Federico Lopez-Moya[1], David Kowbel[2], Mª José Nueda[3], Javier Palma-Guerrero[2, 4], N.
4 Louise Glass[2] and Luis Vicente Lopez-Llorca[1].

5 [1]Laboratory of Plant Pathology, Multidisciplinary Institute for Environmental Studies
6 (MIES) Ramon Margalef, Department of Marine Sciences and Applied Biology,
7 University of Alicante, E-03080 Alicante, Spain.

8 [2]Department of Plant and Microbial Biology, University of California, Berkeley CA,
9 94720-3120 USA.

10 [3]Statistics and Operation Research Department, University of Alicante, E-03080
11 Alicante, Spain.

12 [4]Current address: Department of Environmental Systems Science, ETH Zurich, Zurich,
13 Switzerland.

14 **Authorship emails**:

15 federico.lopez@ua.es

16 djkowbel@berkeley.edu

17 mj.nueda@ua.es

18 javier.palma@usys.ethz.ch

19 lglass@berkeley.edu

20 lv.lopez@ua.es

21

22

23 **Correspondig author:** federico.lopez@ua.es

Molecular BioSystems Accepted Manuscript

View Article Online
DOI: 10.1039/C5MB00649J

Published on 01 December 2015. Downloaded by Universidad de Alicante on 09/12/2015 15:48:54.

24 # Abstract

25 Chitosan is a natural polymer with antimicrobial activity. Chitosan causes plasma
26 membrane permeabilization and induction of intracellular reactive oxygen species
27 (ROS) in *Neurospora crassa*. We have determined the transcriptional profile of *N.*
28 *crassa* to chitosan and identified the main gene targets involved in the cellular response
29 to this compound. Global network analyses showed membrane, transport and
30 oxidoreductase activity as key nodes affected by chitosan. Activation of oxidative
31 metabolism indicates the importance of ROS and cell energy together with plasma
32 membrane homeostasis in *N. crassa* response to chitosan. Deletion strain analysis of
33 chitosan susceptibility pointed, NCU03639 encoding a class 3 lipase, involved in
34 plasma membrane repair by lipid replacement and NCU04537 a MFS monosaccharide
35 transporter related with assimilation of simple sugars, as main gene targets of chitosan.
36 NCU10521, a glutathione S-transferase-4 involved in the generation of reducing power
37 for scavenging intracellular ROS is also a determinant chitosan gene target. Ca^{2+}
38 increased tolerance to chitosan in *N. crassa.* Growth of NCU10610 (*fig 1* domain) and
39 SYT1 (a synaptotagmin) deletion strains was significantly increased by Ca^{2+} in presence
40 of chitosan. Both genes play a determinant role in *N. crassa* membrane homeostasis.
41 Our results are of paramount importance for developing chitosan as antifungal.

42

43

44

45

46 # Keywords

47 Drug targets, time-series analysis, ROS, membrane remodeling, calcium

48

49

Molecular BioSystems Accepted Manuscript

View Article Online
DOI: 10.1039/C5MB00649J

Published on 01 December 2015. Downloaded by Universidad de Alicante on 09/12/2015 15:48:54.

Introduction

Chitosan is a polymer obtained by partial chitin N-deacetylation[1] which has antifungal activity.[2] Chitosan inhibits growth of filamentous fungi and yeast human pathogens.[3,4] To develop chitosan as an antifungal treatment, a full understanding of its mode of action is necessary. In *Saccharomyces cerevisiae,* the response to chitooligosaccharides is mediated by proteins associated with plasma membrane, respiration, ATP production and mitochondrial organization.[5] Five genes (*arl1*, *bck2*, *erg24*, *msg5* and *rba50*) were characterized that provided chitosan resistance when overexpressed or increased sensitivity as a deletion strains. These genes have important roles in signaling pathways, cell membrane integrity and transcription regulation.[5] Other transcriptional studies in *S. cerevisiae* revealed the relevance of oxidative respiration, mitochondrial biogenesis and transport in the response to chitosan.[6] Previous physiological studies in *N. crassa* demonstrated that chitosan causes plasma membrane permeabilization.[7] Membrane fluidity is a key factor determining chitosan sensitivity in fungi.[8] Cell energy and mitochondrial activity have also an important role in moderating the antifungal activity of chitosan.[7] The transcriptional response of filamentous fungi to this antifungal remains unknown.

Membrane damage caused by currently used antifungals (eg. azoles) is associated with the induction of intracellular reactive oxygen species (ROS).[9,10] We have recently shown that low chitosan concentration increased intracellular ROS levels in *N. crassa* leading to partial membrane permeabilization.[4] Increasing chitosan dose dramatically raised ROS levels causing full membrane permeabilization and subsequent cell death. Oxidative stress by chitosan is mediated by the energetic status of the cell. A reduction in cell energy by blocking the electron transport chain protected *N. crassa* from chitosan damage.[7] The plasma membrane of *N. crassa* contains high levels of polyunsaturated free fatty acids (FFA), this fact is directly associated with its susceptibility to chitosan.[8] Fungal plasma membrane lipids could be easily oxidized by an induction of intracellular oxidative stress generated by chitosan as found for other antifungals.[10,11] This fact would link ROS and membrane homeostasis biology in the mode of action of chitosan.

Molecular BioSystems Accepted Manuscript

View Article Online
DOI: 10.1039/C5MB00649J

Published on 01 December 2015. Downloaded by Universidad de Alicante on 09/12/2015 15:48:54.

81 Ca^{2+} is known to be involved in plasma membrane repair.[12] Previous molecular
82 studies revealed SYT1, a synaptotagmin, involved in membrane repair in several
83 organisms[13] including *N. crassa*.[14] Moreover, Ca^{2+} plays a role in the response to
84 oxidative stress and programmed cell death in *N. crassa*.[15] PRM1 and FIG1 are key
85 proteins in calcium-dependent plasma membrane remodeling during membrane fusion
86 in *S. cerevisiae* and *N. crassa*.[16-19] In *N. crassa,* two additional proteins, LFD1 and
87 LFD2 are also involved in Ca^{2+}-dependent plasma membrane repair during cell
88 fusion.[14,20] It is currently unknown, however, how fungi repair membrane damage
89 caused by chitosan.
90
91 In this work, we analyzed the transcriptional response of *N. crassa* germinating
92 conidia and determined the main gene functions related with the exposure to chitosan.
93 We applied temporal series analysis (Next-maSigPro[21] and ASCA-genes[22]) and a
94 network analysis approach (Cytoscape)[23] to understand the dynamics of functions and
95 gene targets involved in *N. crassa* response to chitosan. This study has pointed
96 mitochondrion (ROS) and membrane homeostasis as the main functions in the response
97 of *N. crassa* to chitosan and has identified key gene targets. Deletion strains of these
98 key genes were evaluated for fitness and growth. We further demonstrated that
99 extracellular calcium protects fungal cells from damage caused by chitosan. These
100 studies are a key step for improving the knowledge on the mode of action of chitosan,
101 which is essential for its future development as antifungal.

102 Results and Discussion

103 Chitosan causes an early activation and late repression of *N. crassa* genes

104 The experimental conditions for analyzing the effect of chitosan on *N. crassa*
105 germination and development are shown in Fig. 1. Time-course of *N. crassa* conidia
106 germination is included in Figure 1A. Germination defects were quantified after 8h
107 exposure of *N. crassa* conidia to 0.5 µg ml^{-1} chitosan (Fig. 1B; IC_{50}) which showed an
108 approximately 50% reduction in germination. This chitosan concentration was used for
109 high throughput transcriptomic study.

Molecular BioSystems Accepted Manuscript

View Article Online
DOI: 10.1039/C5MB00649J

Published on 01 December 2015. Downloaded by Universidad de Alicante on 09/12/2015 15:48:54.

110 To identify transcriptional changes caused by exposure of *N. crassa* to chitosan a 3-
111 stage time-course (4, 8 and 16h post-inoculation) was performed. A total of 523 *N.*
112 *crassa* genes were considered differentially expressed (p-value < 0.05), with a fold
113 change ≥ 2 (lower fold change values were considered non-significant), in response to
114 chitosan (Fig. 2A). Of these, 55.6% (291 genes) were down-regulated and 45.3% (237
115 genes) up-regulated. Our time-course experiment showed a progressive reduction in the
116 number of genes whose expression increased upon exposure to chitosan (142 induced
117 genes at 4h, 119 at 8h and 45 at 16h; Fig. 2B). In contrast, exposure to chitosan resulted
118 in an increase in the number of genes whose expression levels decreased over time (79,
119 93 and 207 genes down-regulated at 4, 8 and 16h, respectively; Fig. 2C). A subset of 22
120 genes was differentially expressed consistently (p-value < 0.05; $\log_2$foldchange ≥ 2)
121 throughout the whole time-course (Fig. 2A). Most of these genes (19) were down-
122 regulated, two genes were up-regulated and only one gene of this set (NCU05018) had
123 an early (4 and 8h) induction and a late (16h) gene repression (Fig. 2D).

124 Expression of 10 *N. crassa* genes representative of functional categories that were
125 differentially expressed by exposure to chitosan were selected to validate our RNA-seq
126 analysis. Gene expression was evaluated by qRT-PCR following an 8h exposure to
127 chitosan (Fig S1). These genes were NCU05134, NCU06123, NCU07610, NCU01382
128 and NCU05712 (involved in response to oxidative stress), NCU02363 (involved in
129 response to chemical compounds), NCU05018, NCU3494 *pin-c* (related with
130 heterokaryon incompatibility and membrane biology), NCU05764 (a sam-dependent
131 methyltransferase) and a transcription factor with a zinc-finger domain (NCU05767).
132 All genes analyzed by qRT-PCR showed an expression pattern consistent with that
133 derived from RNA-seq data analysis (Fig. S1).

134 ***N. crassa* main gene functions differentially expressed with chitosan are**
135 **oxidoreductase activity, membrane homeostasis and microtubule organization.**

136 A gene ontology (GO) functional annotation of *N. crassa* genes differentially expressed
137 in response to chitosan was carried out using Blast2GO (Fig. 3 and Figs. S2 and S3). All
138 GO-domains (molecular function, MF; biological process, BP; cell component, CC) and
139 times were considered together for a complete functional gene expression analysis (Fig.

Molecular BioSystems Accepted Manuscript

View Article Online
DOI: 10.1039/C5MB00649J

Published on 01 December 2015. Downloaded by Universidad de Alicante on 09/12/2015 15:48:54.

140 3A). Oxidoreductase activity (70 genes), membrane (57 genes) and transport (44 genes)
141 were the most enriched GO-terms.

142 Using maSigFun software for RNA-seq data time series analysis combined with GO
143 annotation, we generated the time-course of functional gene expression for the most
144 significantly enriched GO-terms representing *N. crassa* response to chitosan (Fig. 3B).
145 The analysis identified 12 significant GO-terms using FDR=0.05 and R^2=0.4 levels, as
146 suggested in previous studies[24]. Chitosan modified patterns of expression of ROS-
147 related GO terms mitochondrion and peroxisome organization (Fig. 3B). Mitochondrion
148 genes increased expression through time reaching maximum values of expression at
149 16h, suggesting that chitosan enhances synthesis/turnover of mitochondrion components
150 (respiration). Genes associated with peroxisome organization, involved in ROS
151 degradation and catabolism of free fatty acids, were first highly expressed (4h) then
152 completely repressed (16h). Likewise, chitosan modified patterns of expression of GO
153 categories related with membrane structure and biology. Exposure to chitosan was
154 associated with repression at 16h of genes involved in cell cortex, vesicle organization
155 and conjugation (Fig. 3B). Moreover, G-protein coupled receptor signaling were
156 compromised by chitosan during all the time-course study (Fig. 3B). These features
157 indicate that chitosan significantly compromised both structure and signaling associated
158 with cell membrane homeostasis. Genes associated with GO-terms related to cell
159 growth such as microtubule organizing center and motor activity had decreased
160 expression values by chitosan through time (Fig. 3B). This behavior suggests the
161 importance of cytoskeleton in the antifungal action of chitosan. Conversely, chitosan
162 increased expression of genes associated with GO terms involved in protein synthesis
163 (ribosome and ribosome biogenesis, Fig. 3B). This would support the increasing
164 expression of genes and synthesis of proteins related to oxidoreductase activity by
165 chitosan (Fig. 3A). In a similar way, nucleolus and structural molecule activity (Fig. 3B)
166 genes were also late activated by chitosan.

167 **Potential gene targets of *N. crassa* to chitosan and their dynamics of expression**

168 Initial time-course analysis showed 5% of *N. crassa* genes significantly expressed in
169 response of *N. crassa* to chitosan. A subset of 33 genes with a relevant change (*p*-value

Molecular BioSystems Accepted Manuscript

View Article Online
DOI: 10.1039/C5MB00649J

170 < 0.05; log_2fold-change > ±4.5) of expression is shown in Table S1. A restrictive cut-off
171 was applied with the aim of detect the genes with large change in expression in response
172 to chitosan. This subset included the 22 genes found in the differential gene expression
173 analysis (Fig. 2) plus genes highly expressed (at early or late steps) associated with
174 enriched GO-terms after chitosan exposure.

175 When applying ASCA-genes method we focused on submodel (b+ab) that represents
176 67.18% of total variation. Two components were selected, explaining 93% of this
177 variability (52.38% and 40.62%, respectively; Fig. S4). They, therefore, represented the
178 main gene expression in response to chitosan. First component identified a gene
179 expression difference between chitosan and control constant through time (Fig. S4A).
180 Second component identified expression pattern characterized by a clear interaction
181 through time (Fig. S4B). The analysis of the squared prediction error (SPE) and
182 leverage, determined a cut-off using gamma method, revealed 410 genes which
183 followed the selected components (which explained 93% of variation) and 474 with a
184 behaviour not identified in these (Fig. S5). Comparisons between ASCA and the fold-
185 change gene selection methods (523 genes in total) revealed 447 genes in common (Fig.
186 S4C). Summarizes graphically this comparison where is observed a high overlap
187 between fold-change gene selection and genes with high leverage (also scores can be
188 observed). Moreover 33 genes with a relevant change (listed in Table S1) were also
189 identified showing high scores for the two components identified after PCA (Fig.S4C).

190 To inspect ASCA gene selection time series two cluster analyses were applied: one
191 to the well-modelled genes (M) and another to the bad-modelled genes (NM) obtaining
192 4 and 6 clusters respectively (Fig4 and S6). Both analyses were performed with the
193 hierarchical method. Cluster 1M (Fig. 4A) contained genes associated with an early
194 response to chitosan including two dioxygenases: NCU01849, the most highly
195 expressed gene in response to chitosan (11.16 fold-induction) and NCU01071 a
196 predicted 2OG-Fe dioxygenase, both involved in response to oxidative stress.

197 We also found a set of genes mainly associated with plasma membrane, signaling
198 and response to chemical compound (NCU02363; RTA1-like protein). In addition, a
199 plasma membrane protein (*het* domain) associated with intracellular oxidative stress

Published on 01 December 2015. Downloaded by Universidad de Alicante on 09/12/2015 15:48:54.

Molecular BioSystems Accepted Manuscript

View Article Online
DOI: 10.1039/C5MB00649J

Published on 01 December 2015. Downloaded by Universidad de Alicante on 09/12/2015 15:48:54.

Molecular BioSystems Accepted Manuscript

200 (NCU07840), hypothetical protein with a C-terminal homeodomain (NCU00733) and
201 hypothetical protein with a peroxisome membrane anchored protein conserved region
202 (NCU04555) which strongly decreased in expression levels in *N. crassa* conidia treated
203 with chitosan. Cluster 4M showed a steady increase of gene expression (Fig. 4D).
204 Genes in this cluster were involved in cell response to oxidative stress (NCU05134 and
205 NCU08907) and a monosaccharide transporter perhaps involved in chitosan
206 assimilation or detoxification (NCU04537, fold-induction 9.27 after 16h growing with
207 chitosan). Besides, other genes related with sugars assimilation were also induces in
208 presence of chitosan such as NCU01633 (*hxt13*; Table S2). Clusters 2M and 3M, had
209 gene expression changes in the control but not in the chitosan treatment (Figs. 4B and
210 4C). Genes in these clusters were mainly related with fungal reproduction and
211 development and response to oxidative stress. Cluster 2M included two genes
212 associated with membrane homeostasis: NCU03494 (*pin-c*) essential for non-self-
213 recognition and NCU10610, a protein with a *fig 1* domain (Ca^{2+} regulator and
214 membrane fusion) related with cell fusion.

215 Genes which did not fit the model (NM), with high SPE and leverage in the ASCA
216 analysis, were grouped in 6 clusters including 474 genes (Fig. S6). Cluster 5NM which
217 showed a late activation in presence of chitosan, included genes such as NCU10521
218 (fold-induction 8.16 at 16h) a glutathione S-transferase-4 possibly involved in the
219 generation of reducing power for scavenging intracellular ROS. Other genes involved in
220 ROS assimilation were also induced at 16h such as NCU05780 (*gst-1*; Table S2).
221 Cluster 3NM included expression of genes such as NCU08770 a hypothetical protein
222 with a histone chaperone domain with slight changes of expression in presence of
223 chitosan (Fig. S6). Cluster 4NM included genes with an early induction (4-8h) and then
224 a reduction of gene expression such as NCU03639, a lipase class 3 involved in lipid,
225 fatty acids and isoprenoid metabolism. The overexpression of this gene suggests its role
226 in plasma membrane homeostasis during chitosan damage.

227 Other significantly expressed (more than 6 fold-change expression, Table S2) genes
228 in response to chitosan related with the main functions described previously included
229 NCU03213 encoding a predicted mannosyl-phosphorylation protein related with
230 phosphocholine metabolism (lipid modification). Early induction of other genes related

View Article Online
DOI: 10.1039/C5MB00649J

231 with predicted roles in lipid metabolism such as NCU16960 (geranyl reductase) putative
232 involved in the biosynthesis of plasma membrane lipids were also detected.

233 ***N. crassa* deletion strains involved in membrane homeostasis and ROS**
234 **detoxification showed increased sensitivity to chitosan**

235 Fifteen deletion strains of genes highly expressed and associated with enriched GO-
236 terms in response to chitosan were evaluated to identify gene targets in *N. crassa*. Five
237 deletion strains showed increased sensitivity to chitosan (Fig. 5 and Fig. S7).
238 ΔNCU03639 (lipase) and ΔNCU04537 (monosaccharide transporter) were the most
239 sensitive. These deletion strains exhibited a minimal inhibitory concentration (MIC, 3
240 $\mu g\ ml^{-1}$) lower than the WT (MIC 6 $\mu g\ ml^{-1}$; Fig. 5A). They also showed a 6-8h delay in
241 the start of the exponential growth phase at 2 $\mu g\ ml^{-1}$ of chitosan in comparison to the
242 WT (Figs. 5B-5D). Furthermore, ΔNCU10521 (glutathione S-transferase), ΔNCU08907
243 Clock controller gene 13 (*ccg-13*) and ΔNCU07840 (plasma membrane protein with a
244 *het* domain) were moderately (MIC at 4 $\mu g\ ml^{-1}$) sensitive to chitosan (Fig. 5A). These
245 strains showed a 6-12h delay in the start of exponential growth phase with respect to
246 WT at 3 $\mu g\ ml^{-1}$ of chitosan (Fig. S7). ΔNCU10610 (Ca^{2+} regulator with *fig 1* domain)
247 showed the same MIC as WT (6 $\mu g\ ml^{-1}$), but had a delay (8h) in the start of exponential
248 growth phase at 4 $\mu g\ ml^{-1}$ chitosan (Fig. S7 and Table S3). Conversely, ΔNCU02363
249 (RTA1 like-protein) and ΔNCU05134 (hypothetical protein) with the same MIC as the
250 WT, started their exponential phases 7 and 16h earlier than WT (Fig. S7 and Table S3)
251 indicating moderate tolerance of chitosan respect to WT. ΔNCU08770 (hypothetical
252 protein with a histone chaperone domain CHZ) had increased resistance to chitosan
253 (MIC > 6 $\mu g\ ml^{-1}$; Fig. 5E). The start of the exponential growth phase in this deletion
254 strain was 15h earlier than WT at 4 $\mu g\ ml^{-1}$ of chitosan (Table S3).

255 Thirteen deletion strains (mating type a) were crossed to WT (mating type A) to
256 assess meiotic segregation of chitosan sensitivity phenotype with the hygromycin
257 marker. Seggregants of each mutant showed similar chitosan sensitivity than the
258 original deletion strain. In four chitosan gene targets (ΔNCU03639, ΔNCU04537,
259 ΔNCU07840 and ΔNCU10521), segreggants showed the same chitosan antifungal
260 phenotype (MIC) and hygromycin resistance than the original deletion strains.

Published on 01 December 2015. Downloaded by Universidad de Alicante on 09/12/2015 15:48:54.

Molecular BioSystems Accepted Manuscript

View Article Online
DOI: 10.1039/C5MB00649J

Published on 01 December 2015. Downloaded by Universidad de Alicante on 09/12/2015 15:48:54.

Molecular BioSystems Accepted Manuscript

261 **Ca^{2+} protects *N. crassa* conidia from chitosan damage**

262 Ca^{2+} increased tolerance to chitosan in *N. crassa* (Fig. 6). The WT strain at 0.68 mM
263 $CaCl_2$ with 0.5 µg ml^{-1} chitosan resumed growth 4h earlier than without Ca^{2+} (Figs. 6A).
264 A higher level of $CaCl_2$ (2.72 mM) in the presence of 0.5 µg ml^{-1} chitosan further
265 improved fungal growth with a 7h advance in the start of the exponential phase with
266 respect to *N. crassa* with chitosan and no calcium (Fig. 6A). Increasing $CaCl_2$
267 concentrations with no chitosan did not affect fungal growth (data not shown).

268 Conidia in calcium-free medium treated with chitosan (0.5 µg ml^{-1}) were stained
269 (Fig. 6B) with the vital dye propidium iodide (PI) indicating cell mortality. On the
270 contrary, conidia treated with both chitosan (0.5 µg ml^{-1}) and calcium chloride (0.68
271 mM), this showed no staining remaining alive (Fig. 6C). Similar results were found
272 when increasing chitosan concentrations (Fig. S8). In particular, 0.5, 2.5 and 5 µg ml^{-1}
273 chitosan and $CaCl_2$ treated cells had significantly (p-value < 0.05) lower mortality than
274 conidia treated with chitosan but no calcium.

275 Treatment with Ca^{2+} also reduced chitosan damage in deletion strain in the locus
276 ΔNCU10610 with a *fig 1* domain and ΔNCU03263 (*syt-1*), both associated with plasma
277 membrane remodeling (Figs. 6D and 6E). Increasing $CaCl_2$ concentration (10 mM to 20
278 mM) significantly improved growth of WT, ΔNCU10610 and ΔNCU03263 strains in a
279 medium amended with a high amount of chitosan (4 µg ml^{-1}; Figs. 6D and 6E). With
280 less concentration of Ca^{2+} in the medium (0.68 mM), chitosan completely inhibited
281 fungal growth. ΔNCU10610 showed more tolerance to chitosan respect to WT, this
282 strain started exponential phase at 27h, whereas WT strain did so 3h later under the
283 same conditions. ΔNCU03263 was most sensitive to chitosan with high amount of
284 calcium, starting the exponential phase after 35h, with slower growth than WT and
285 ΔNCU10610. When [$CaCl_2$] was increased (20 mM) all strains tested showed higher
286 resistance to chitosan (Fig. 6E). This was especially relevant for ΔNCU03263 which
287 showed a ca. 2 fold growth increase under these conditions (Fig. 6E).

288

View Article Online
DOI: 10.1039/C5MB00649J

Published on 01 December 2015. Downloaded by Universidad de Alicante on 09/12/2015 15:48:54.

289 We found in this work that chitosan significantly induced changes of expression of
290 5% of *N. crassa* genes in the genome. A global Cytoscape network showed membrane
291 and transport as key nodes grouping genes affected by chitosan (Fig. 7). Plasma
292 membrane was connected with cell vesicles and cell wall suggesting the importance of
293 these outer structures and their dynamics in presence of chitosan. Oxidoreductase
294 enhanced node indicated the importance of ROS and cell energy in *N. crassa* response
295 to chitosan.[4,7] Several nodes related with cytoskeleton dynamics indicate that chitosan
296 also affects cell growth (Fig. 7). Other transcriptional studies, using *S. cerevisiae*
297 mutant collections determined genes associated with plasma membrane, respiration,
298 ATP production and mitochondrial organization as main targets of
299 chitooligosaccharides.[5,6]

300 In this study, we demonstrated that exposure to chitosan increased the expression of
301 genes involved in plasma membrane dynamics such as lipases. Imidazoles and triazoles
302 (e.g. fluconazole, voriconazol and others) mode of action is based on the ergosterol
303 biosynthesis inhibition,[25,26] thereby altering plasma membrane fluidity. Chitosan is also
304 an antifungal affecting plasma membrane. Fungi with enriched unsaturated free fatty
305 acids in their plasma membrane (increased fluidity) are sensitive to chitosan (e.g. *N.*
306 *crassa*). In contrast, fungi with less unsaturated free fatty acids in their membranes (low
307 fluidity) such as the nematophagus fungus *Pochonia chlamydosporia,* are resistant to
308 chitosan.[8,27] In our work, we show that chitosan activates genes related with plasma
309 membrane homeostasis such as the class 3 lipase NCU03639 (Fig. 8). The increase on
310 chitosan sensitivity of NCU03639 deletion strain and the induction of genes related with
311 free fatty acid plasma membrane remodeling such as NCU16960 (geranyl reductase),
312 suggests their role in lipid replacement. This group of genes is mainly associated with
313 plasma membrane stabilization by changes in free fatty acid composition caused by
314 other abiotic stresses.[28] Furthermore, chitosan also activated genes related with vesicular
315 transport, which is associated with lipid transfer.[29]

316 Moreover, chitosan also induced expression of *N. crassa* genes related with
317 movement of molecules through plasma membrane such as MFS transporters. The
318 activation of a monosaccharide transporter and other genes related with exchange of
319 molecules is one of the general responses of *N. crassa* to chitosan. Transport activation

Molecular BioSystems Accepted Manuscript

View Article Online
DOI: 10.1039/C5MB00649J

Published on 01 December 2015. Downloaded by Universidad de Alicante on 09/12/2015 15:48:54.

320 is a widely described response of several filamentous fungi and yeast in response to
321 antifungals.[30] *C. albicans* activates genes involved in transport and molecule trafficking
322 in presence of ketoconazole.[31] Susceptibility to azoles has been likely found due to a
323 reduced efflux activity of pumps.[32] Likewise, amphotericin B induces expression of
324 high-affinity glucose transporters (MFS transporters) and permeases encoding genes in
325 *S. cerevisiae*.[30] In our study, *N. crassa* NCU04537 deletion strain, encoding a
326 monosaccharide transporter, showed an increase in chitosan sensitivity, suggesting a
327 determinant role of this protein in the assimilation of glucosamine and N-acetyl
328 glucosamine monomers.[33]

329 Currently used antifungals, as well as chitosan, induce intracellular oxidative stress
330 affecting plasma membrane permeability. This may be associated with an imbalance of
331 intracellular redox state.[4,10] An increase in the intracellular ROS is a general response to
332 several antifungals and antimicrobial peptides which target the plasma membrane.[9,34]
333 We have also recently demonstrated that chitosan elicited a rise in ROS coincident with
334 the start of plasma membrane permeabilization.[4] In this paper we have demonstrated
335 that chitosan induced the expression of genes encoding mono- and dioxygenases and
336 other proteins related with ROS homeostasis. Other antifungals (e.g. rotenone and
337 staurosporine) also increase levels of intracellular oxidative stress associated with
338 subsequent cellular death.[35,36] Increase in associated ROS by chitosan could induce
339 plasma membrane free fatty acid oxidation and formation of oxylipins.[37] These would
340 damage plasma membrane and cause its subsequent permeabilization.[38] In our study,
341 when NCU10521, encoding a glutathione S-transferase (GST), was eliminated
342 sensitivity of *N. crassa* to chitosan increased. GST is known to deaden ROS by-
343 products such as peroxidized lipids.[39] This suggests a link between ROS and membrane
344 damage in the mode of action of chitosan (Fig. 8). Other antifungals also induce
345 glutathione enzymes to reduce intracellular ROS levels in *N. crassa*.[40]

346 We have discovered that chitosan inhibits gene functions related with cytoskeleton
347 dynamics such as microtubule organization and motor activity. Increased levels of
348 intracellular ROS in *Magnaporthe oryzae* caused F-actin depolymerization affecting
349 hyphal polar growth.[41] In *N. crassa* deletion of a NOX gene encoding a NADPH
350 oxidase results in reduction of hyphal growth.[42] These observations support the

Molecular BioSystems Accepted Manuscript

View Article Online
DOI: 10.1039/C5MB00649J

Published on 01 December 2015. Downloaded by Universidad de Alicante on 09/12/2015 15:48:54.

351 hypothesis that an increase in intracellular ROS causes an abnormal distribution of F-
352 actin. Cytoskeleton disorganization could then be one of the mechanisms by which
353 chitosan inhibits fungal growth. The oxidative stress and associated phenomena such as
354 free fatty acid peroxidation or F-actin polymerization could be directly involved in
355 chitosan antifungal activity.

356 It is known that the balance between Ca^{2+} and ROS affects intracellular signaling and
357 cell homeostasis.[43] We have demonstrated that Ca^{2+} is involved in *N. crassa* tolerance to
358 chitosan. Ca^{2+} is also involved in the increasing threshold of *N. crassa* to antifungals
359 such as staurosporine.[44] Calcium plays a role in the mechanisms of plasma membrane
360 remodeling in *S. cerevisiae* budding[45] and during cell fusion in *N. crassa*.[14,17] In this
361 work, we report NCU10610 (Ca^{2+} regulator with *fig 1* domain) significantly repressed
362 by chitosan. The presence of a *fig 1* domain suggests its role as Ca^{2+} regulator in cell
363 fusion. In view of the relevance of this phenomenon in plasma membrane remodeling,
364 we have also evaluated the role of SYT1 in the mechanisms of plasma membrane
365 remodeling mediated by Ca^{2+}. SYT1 may be involved in membrane damage restored
366 during fusion of germlings in *N. crassa*.[14] In our study Δ*syt1* had increased sensitivity to
367 chitosan. When Δ*syt1* was exposed to chitosan together with Ca^{2+} (10 mM) we found
368 increased sensitivity of this deletion strain to chitosan respect to WT. This would be
369 associated with the capability of this gene to trigger mechanisms of plasma membrane
370 damage repair mediated by Ca^{2+}. Besides, high levels of extracellular Ca^{2+} (20 mM),
371 highly reduced chitosan damage in Δ*syt1*. This deletion strain grow with the same
372 fitness that the WT under these conditions. This would be associated with the activation
373 of other *N. crassa* genes involved in plasma membrane remodeling mediated by Ca^{2+}.
374 Our results would suggest the importance of Ca^{2+} on the mechanisms of plasma
375 membrane remodeling after chitosan damages.

376 Conclusion and outlook

377 This work provides the first study of the gene expression response of a filamentous
378 fungus (*N. crassa*) to chitosan. Transcriptomics revealed oxidoreductase activity,
379 membrane homeostasis and microtubule organization as the main gene functions
380 differentially expressed. We identified a class 3 lipase, a MFS monosaccharide

Molecular BioSystems Accepted Manuscript

View Article Online
DOI: 10.1039/C5MB00649J

381 transporter and a glutathione transferase as main gene targets of chitosan in *N. crassa*.
382 Our study opens new possibilities to study gene pathways involved in membrane
383 remodeling after chitosan damage with a relevant role of Ca^{2+}. These studies are a key
384 step to develop chitosan as antifungal drug in the future. Our results could help to
385 identify the main gene targets of chitosan in medical important fungi.

Published on 01 December 2015. Downloaded by Universidad de Alicante on 09/12/2015 15:48:54.

386 Methods

387 Growth conditions

388 *Neurospora crassa* wild-type strain was 74-OR23-IVA (FGSC2489) and the deletion
389 strains were generated by the *Neurospora* Genome Project[46,47] and kindly provided by
390 the Fungal Genetics Stock Center (FGSC, Kansas, USA)[48] are shown in Table S1.
391 Strains were grown on Vogel's minimal medium agar (VMMA) (1x Vogel's salts, 2%
392 sucrose and 1.5% technical agar).

393 Chitosan

394 A medium molecular weight chitosan (70 kDa) with an 82.5% deacetylation degree
395 (T8s; Marine BioProducts GmbH; Bremerhaven, Germany) was used. Chitosan was
396 prepared as described in Palma-Guerrero *et al.*, 2008.[27]

397 Germinating conditions and time-course of *N. crassa* sensitivity to chitosan

398 To determine the optimal medium to assess the behavior of *N. crassa* exposed to
399 chitosan, three variants of the Vogel's minimal medium were evaluated (VMM). These
400 media were standard VMM (1x salts, 2% sucrose), VMM salts diluted 100 times with
401 2% sucrose and VMM salts diluted 100 times and 0.02% sucrose. We finally adopted
402 the second one because chitosan precipitated with some salts included in standard
403 VMM. Time-course experiments of germination were assessed every 2h for 24h under
404 continuous light, shaking at 200 rpm and 25ºC.

405 *N. crassa* conidia sensitivity to chitosan was evaluated using selected media, with
406 sub-lethal concentrations of chitosan (0.1-1 μg ml^{-1}). The percentage of *N. crassa*
407 conidial germination with chitosan for 2, 4, 6, 8, 10, 12 and 16h after inoculation was

Molecular BioSystems Accepted Manuscript

View Article Online
DOI: 10.1039/C5MB00649J

408 measured. We selected a chitosan dose that resulted in a 50% inhibition of germination
409 respect to the control (IC_{50}).

410 **RNA extraction and cDNA synthesis.**

411 From *N. crassa* cultures in contact with chitosan and controls (without chitosan) for 4,
412 8 and 16h total RNA was isolated using TRIzol reagent (Life Tech) according to the
413 manufacturer's instructions. RNA was then treated with DNase (Turbo DNA-free,
414 Ambion) to eliminate DNA remains. For poly (A+) RNA purification, 10 µg of total
415 RNA was bound to dynal oligo (dT) magnetic beads (Invitrogen) twice, using the
416 manufacturer's instructions. Purified poly (A+) RNA was fragmented by metal-ion
417 catalysis (Ambion) followed by precipitation with 1/10 vol 3M sodium acetate and 3×
418 vol 100% ethanol. Precipitated RNA was 70% ethanol washed and then resuspended
419 into 10.5 µl nuclease free water. For first strand cDNA synthesis, the fragmented poly
420 (A+) RNA was incubated with 3 µg random hexamers (Invitrogen), incubated at 65°C
421 for 5 min and then transferred to ice. First strand buffer (4 µL; Invitrogen),
422 Dithiothreitol (DTT), dNTPs and RNAseOUT (Invitrogen) were added to a final
423 concentration of 1×, 10 mM, 200 µM and 1U/µL, respectively in a final volume of 20 µl
424 and the samples were incubated at 25°C for 2 minutes. Superscript II (200 U;
425 Invitrogen) were added and the samples were incubated at 25°C for 10 min, 42°C for 50
426 min and 70°C for 15 min. For second strand synthesis, 51 µL of H_2O, 20 µL of 5×
427 second strand buffer (Invitrogen), and dNTPs (10 mM) were added to the first cDNA
428 strand synthesis mix and incubated on ice for 5 min. RNaseH (2 U; Invitrogen), DNA
429 pol I (50 U; Invitrogen) were then added and the mixture was incubated at 16°C for
430 2.5h.

431 **Library construction and sequencing**

432 End-repair was performed by adding 45 µL of H_2O, T4 DNA ligase buffer with 10 mM
433 ATP (NEB; 10 µL), dNTP mix (10 mM), T4 DNA polymerase (15 U; NEB), Klenow
434 DNA polymerase (5 U; NEB), and T4 PNK (50 U; NEB) to the sample and incubating
435 for 30 min at 20°C. A single base was added each to cDNA fragment by adding Klenow
436 buffer (NEB), dATP (1 mM), and Klenow 3′ to 5′ exo- (15 U; NEB). The mixture was
437 then incubated at 37°C for 30 min. Standard Illumina adapters (FC) were ligated to the

Published on 01 December 2015. Downloaded by Universidad de Alicante on 09/12/2015 15:48:54.

Molecular BioSystems Accepted Manuscript

View Article Online
DOI: 10.1039/C5MB00649J

438 cDNA fragments using 2× DNA ligase buffer (Enzymatics), 1 μL of adapter oligo mix
439 and DNA ligase (5 U; Enzymatics). The sample was incubated at 25°C for 15 min. The
440 sample was purified in a 2% low-melting point agarose gel, and a slice of gel containing
441 200-bp fragments was removed and the DNA purified. The polymerase chain reaction
442 (PCR) was used to enrich the sequencing library. A 10 μL aliquot of purified cDNA
443 library was amplified by PCR using the pfx DNA polymerase (2 U; Invitrogen) and
444 with 1 μl of genomic primers 1.1 and 2.1 (Illumina). PCR cycling conditions included a
445 denaturing step at 98°C for 30 sec, 12 cycles of 98°C for 10 sec, 65°C for 30 sec, 68°C
446 for 30 sec, and a final extension at 68°C for 5 min. All libraries were sequenced on a
447 HiSeq 2000 platform to a depth of over 190 million 50 bp reads using standard Illumina
448 operating procedures.

449 **Transcript abundance, annotation and functional analysis.**

450 Sequenced libraries were mapped against predicted transcripts from the *Neurospora*
451 *crassa* OR74A genome (v10) with TopHat (v2.0.4)[49] and the short sequence aligner
452 Bowtie (v2.0.0.6).[50] Transcript abundance measured as FPKMs (Fragments Per
453 Kilobase transcript model per Million fragments mapped) was calculated with Cufflinks
454 (v 2.0.2) using counts that exclusively mapped to predicted transcripts to estimate the
455 FPKM denominator. Genes which had a differential expression cut-off of p-value <
456 0.05 (we adjusted p-value as the Benjamini Hochberg filter; q value in TopHat; to adjust
457 for the false discovery rate) between control and sample were used for further analysis.
458 In the fold change analysis a lo_2foldchange ≥ 2 was adopted to characterize the main
459 gene functions and genes involved in the response of *N. crassa* to chitosan. The project
460 of *N. crassa* gene expression profile in response to chitosan has been deposited in
461 NCBI's Gene Expression Omnibus[51] and is accessible through GEO Series accession
462 number GSE75293 (https://www.ncbi.nlm.nih.gov/geo/query/acc.cgi?acc=GSE75293).

463 *N. crassa* transcript sequences were re-annotated using Blast2GO software (Version
464 2.7.1) to improve the standard annotation provided by the Broad *N. crassa* genome
465 (http://www.broadinstitute.org/annotation/genome/neurospora/MultiHome.html), a
466 consensus set of transcripts were functionally annotated (gene ontology, GO) using
467 Blast2GO (http://www.blast2go.com/b2ghome).[52] Gene families were established using

Published on 01 December 2015. Downloaded by Universidad de Alicante on 09/12/2015 15:48:54.
Molecular BioSystems Accepted Manuscript

View Article Online
DOI: 10.1039/C5MB00649J

Published on 01 December 2015. Downloaded by Universidad de Alicante on 09/12/2015 15:48:54.

468 the InterPro (http://www.ebi.ac.uk/interpro) and KEGG databases
469 (http://www.genome.jp/kegg/pathway.html). For *N. crassa* gene annotation we also
470 used several tools, HMMR[53] including Pfam, TIGRFAM, Gene 3D and Superfamily
471 databases. In addition, Wolf PSORT[54] was used to obtain information about domains
472 and cellular gene localizations. Gene annotations were finally examined using
473 BLASTp.[55]

474 **RNA-seq time-series data analysis**

475 Significant differential gene expression changes over time were assessed by applying
476 the maSigPro R package[21] to the groups of genes included in each functional GO
477 category. This approach was described, as an adaptation of maSigPro[56] named
478 maSigFun[24] for microarray data. This algorithm has been updated for RNA-seq data in
479 this work. The maSigPro method follows a two-stage regression strategy to identify
480 genes with significant changes in expression over time. False discovery rate (FDR) and
481 R^2 level as measure of the good of fit of the regression model are the factors for gene
482 selection. Finally the package includes several clustering algorithms and visualization
483 tools available to group and display the selected gene-profiles.

484 Transcriptional responses of interest were detected with the application of ASCA-
485 genes method.[22] Considering an experiment with 2 factors (a and b, usually time and the
486 experimental group, in our case chitosan treatment), data can be collected in a data
487 matrix X, where rows represent samples and columns represent genes. ASCA first
488 decomposes X into matrices (X_a, X_b and X_{ab}) with the estimates of the ANOVA
489 (Analysis of Variance) parameters: X_a contains the time effects, X_b treatment effects
490 and X_{ab} the interactions, obtained gene by gene. When the main interest of a study is the
491 identification of genes with differences in the experimental groups, X_b is joined to X_{ab}.
492 Principal Component Analysis (PCA) is then applied on each of these matrices to
493 summarize the information of each source of variation and giving as a result two PCA
494 analyses that are called submodels. ASCA-genes compute the main patterns of variation
495 and two statistics for each gene in each submodel: leverage and the squared-prediction
496 error (SPE). Leverage indicates the importance of a gene in the main behavior
497 discovered. SPE quantifies the variability of a gene that is not detected for the model.

Molecular BioSystems Accepted Manuscript

View Article Online
DOI: 10.1039/C5MB00649J
Published on 01 December 2015. Downloaded by Universidad de Alicante on 09/12/2015 15:48:54.
Molecular BioSystems Accepted Manuscript

498 Focusing on these measures, ASCA-genes provides two lists of genes: the first one with
499 genes that follow the main general patterns. The second one including genes with odd
500 behaviors or outlier data. To obtain this gene selection the gamma method[57] was
501 applied.

502 **Real time quantitative PCR for RNA-seq validation**

503 cDNA was synthetized with a retro-transcriptase RevertAid (Thermo) using oligo dT
504 (Thermo). Gene expression was quantify using real-time reverse transcription PCR
505 (qRT-PCR), SYBR Green with ROX (Roche) were used following the manufacturer's
506 instructions. Gene quantifications were performed in a Step One Plus real-time PCR
507 system (Applied Biosystems). Relative gene expression was estimated with the ΔΔCt
508 methodology,[58] with three technical replicates per condition. Primers used to quantify
509 the expression of genes related with *N. crassa* response to chitosan are shown in Table
510 S4. Expression of the TATA-binding protein (NCU04770) and transcription elongation
511 factor S-II (NCU02563) were used as endogenous controls for all experiments, since
512 these genes showed Ct stability for all conditions tested.

513 **Evaluation of selected deletion strains to determine the genes involved in the**
514 **response of *N. crassa* to chitosan**

515 Experiments in liquid media were set to evaluate growth kinetics of *N. crassa* (WT) and
516 selected homokaryons deletion strains (Table S1). *N. crassa* conidia were obtained from
517 8-10 day-old sporulated cultures, by adding 2 ml of distilled water. The resulting
518 conidial suspensions were then filtered through Miracloth (Calbiochem) to remove
519 hyphal fragments. Conidial suspensions were adjusted to a final concentration of 10^6
520 conidia ml^{-1} with 1/100 VMM salts and 2% sucrose.

521 Chitosan (1-6 µg ml^{-1}) was added to the medium and 200 µL per well were dispensed
522 into 96 well microtiter plates (Sterillin Ltd., Newport, UK). Plates were inoculated with
523 *N. crassa* conidia (2×10^5 conidia per well) and then incubated at 25 ºC during 48h in a
524 GENios^{TM} multiwell spectrophotometer (Tecan, Männedorf, Switzerland) in the dark.
525 The chitosan effect on growth of *N. crassa* strains was evaluated by measuring optical
526 density at 490 nm (OD_{490}).[4] In order to identify the antifungal activity of chitosan on *N.*

View Article Online
DOI: 10.1039/C5MB00649J

Published on 01 December 2015. Downloaded by Universidad de Alicante on 09/12/2015 15:48:54.

527 *crassa* strains, we applied a spot assay in SFG medium (2% sorbose, 0.05% glucose and
528 fructose and 1.5% agar).[59]

529 Growth in presence of the same concentration of deletion strains (mating type a) to
530 chitosan was confirmed by segregation analysis.[60] Ascospore progeny were selected
531 from crosses with FGSC 2489 (mating type A). Seggregants were tested both for
532 chitosan and hygromycin sensitivity. The latter was tested in all deletion strains used in
533 this work. Seggregants had the same chitosan sensitivity than the original deletion strain
534 and were hygromycin (200 µg ml^{-1}) resistant.

535 **Evaluation of the effect of Ca^{2+} in the response of *N. crassa* to chitosan**

536 To evaluate the effect of Ca^{2+} on conidia treated with chitosan, we exposed *N. crassa*
537 conidia (10^6 conidia ml^{-1}) to chitosan (0.5 µg ml^{-1}) with either 0.17; 0.34; 0.68; 1.36 or
538 2.72 mM $CaCl_2$. Growth kinetics was evaluated in a 96-multiwell microplate by
539 measuring optical density at 490 nm for 48h, as described above.

540 Viability of conidia was determined using propidium iodide (PI; Sigma)[7] after
541 exposure to chitosan (0.5 µg ml^{-1}), and $CaCl_2$ at 0.68 mM, conidia without $CaCl_2$ were
542 used as a controls for this compound. *N. crassa* conidia were treated with chitosan for 2
543 h and then labeled with 2 µg ml^{-1} PI to evaluate cell viability. Fluorescence in conidia
544 was assessed using an Olympus BH-2 fluorescence microscope with 488 nm and 560
545 nm as excitation and detection wavelengths, respectively, and then photographed with a
546 Leica DFC480 digital camera (Leica Microsystems, Wetzlar, Germany).

547 The effect of higher concentrations of Ca^{2+} (10 and 20 mM) on WT and two deletion
548 strains, ΔNCU10610 (Ca^{2+} regulator with *fig 1* domain) and ΔNCU03263 (*syt1*) when
549 combined with chitosan (4 µg ml^{-1}) was also determined.

550 **Cytoscape network of functional gene annotation of *N. crassa* gene response to**
551 **chitosan**

552 For this analysis, we performed functional enrichment analysis with GSEA (Gene Set
553 Enrichment Analysis).[61] The enrichment maps were generated with Enrichment Map
554 Plugin v1.1[62] developed for Cytoscape.[23] Nodes in the maps were clustered with the

Molecular BioSystems Accepted Manuscript

View Article Online
DOI: 10.1039/C5MB00649J

Published on 01 December 2015. Downloaded by Universidad de Alicante on 09/12/2015 15:48:54.

555 Markov clustering algorithm, using an overlap coefficient computed by the plugin as the
556 similarity metric (coefficient < 0.5 were set to zero) and an inflation parameter with
557 value of 2. For each cluster, the leading edge was computed as in Subramanian *et al.*
558 (2005)[61] for each member of a node. A complete functional gene network map of *N.*
559 *crassa* in response to chitosan was finally generated.

560 Acknowledgements

561 This work was supported by the National Institutes of Health (USA) grant GM060468
562 to NLG and Spanish Ministry of Economy and Competitiveness Grant AGL 2011-
563 29297/AGR to LVLL.

564 We thank help from Dr. Maria DLA Jaime (University of National Institutes of
565 Health–NIDDK, Bethesda, USA) with GSEA and Cytoscape analyses. We also thank
566 support from BioBam Bioinformatics (Valencia, Spain) to use Blast2GO Pro. We also
567 wish to thank Ms. Nuria Escudero (University of Alicante) for her critical comments of
568 the manuscript.

569 References

570 1. R.M.N.V. Kumar, *React. Funct. Polym.*, 2000, **46** (1): 1-27.

571 2. C.R. Allan, and L.A. Hadwiger, *Exp. Mycol.*, 1979, **3** (3): 285-287.

572 3. S.N. Kulikov, S.A. Lisovskaya, P.V. Zelenikhin, E.A. Bezrodnykh, D.R. Shakirova,
573 I.V. Blagodatskikh, V.E. Tikhonov, *Eur. J. Med. Chem.*, 2014, **74:** 169-178.

574 4. F. Lopez-Moya, M.F. Colom-Valiente, P. Martinez-Peinado, J.E. Martinez-Lopez,
575 E. Puelles, J.M. Sempere-Ortells, L.V. Lopez-Llorca, *Fun. Biol.*, 2015, **119** (2-3):
576 154-169.

577 5. M.D.L.A. Jaime, L.V. Lopez-Llorca, A. Conesa, A.Y. Lee, M. Proctor, L.E. Heisler,
578 M. Gebbia, G. Giaever, J.T. Westwood, C. Nislow, *BMC Genomics*, 2012, **13** (1):
579 267.

Molecular BioSystems Accepted Manuscript

View Article Online
DOI: 10.1039/C5MB00649J

Published on 01 December 2015. Downloaded by Universidad de Alicante on 09/12/2015 15:48:54.

580 6. A. Zakrzewska, A. Boorsma, S. Brul, K.J. Hellingwerf, F.M. Klis, *Eukaryot. Cell*.,
581 2005, **4** (4): 703–715.

582 7. J. Palma-Guerrero, I.C. Huang, H-B. Jansson, J. Salinas, L.V. Lopez-Llorca, and
583 N.D. Read, *Fungal Genet. Biol*., 2009, **46** (8): 585–594.

584 8. J. Palma-Guerrero, J.A. Lopez-Jimenez, A.J. Pérez-Berná, I. Huang, H-B. Jansson,
585 J. Salinas, J. Villalaín, N.D. Read, L.V. Lopez-Llorca, *Mol. Microbiol*., 2010, **75**
586 (4): 1021-1032.

587 9. M.A. Ghannoum and L.B. Rice, *Clin. Microbiol. Rev*., 1999, **12** (4): 501-517.

588 10. I.E.J.A. François, B.P.A. Cammue, M. Borgers, J. Ausma, G.D. Dispersyn, K.
589 Thevissen, *Antiinfect. Agents Med. Chem*., 2006, **5** (1): 3-13.

590 11. N. Delattin, B.P. Cammue, K. Thevissen, *Future Med. Chem*., 2014, **6** (1): 77-90.

591 12. N.W. Andrews, P.E. Almeida, M. Corrotte, *Trends Cell Biol*., 2014, **24** (12): 734-
592 742.

593 13. K.D. Brewer, T. Bacaj, A. Cavalli, C. Camilloni, J.D. Swarbrick, J. Liu, A. Zhou, P.
594 Zhou, N. Barlow, J. Xu, A.B. Seven, E.A. Prinslow, R. Voleti, D. Häussinger, A.M.
595 Bonvin, D.R. Tomchick, M. Vendruscolo, B. Graham, T.C. Südhof, J. Rizo, *Nat.*
596 *Struct. Mol. Biol*., 2015, **22** (7): 555-564.

597 14. J. Palma-Guerrero, A.C. Leeder, J. Welch, N.L. Glass, *Mol. Microbiol*., 2014, **92**
598 (1): 164-182.

599 15. A.P. Gonçalves, J.M. Cordeiro, J. Monteiro, C. Lucchi, P. Correia-de-Sá, A.
600 Videira, *Biochim. Biophys. Acta*., 2015, **1847** (10): 1064-1074.

601 16. E.M. Muller, N.A. Mackin, S.E. Erdman, K.W. Cunningham, *J. Biol. Chem*.,
602 2003, **278** (40): 38461-38469.

603 17. A. Fleissner, S. Diamond, N.L. Glass, *Genetics*, 2009, **181** (2): 497–510.

604 18. B. Cavinder F. Trail, *Eukaryot. Cell*., 2012, **11** (8): 978-988.

Molecular BioSystems Accepted Manuscript

View Article Online
DOI: 10.1039/C5MB00649J

605 19. M.Á. Curto, M.R. Sharifmoghadam, E. Calpena, N. De León, M. Hoya, C. Doncel,
606 J. Leatherwood, M.H. Valdivieso, *Genetics*, 2014, **196** (4):1059-1076

607 20. J. Palma-Guerrero, J. Zhao, A.P. Gonçalves, T.L. Starr, N.L. Glass, *Eukaryot. Cell*.,
608 2015, **14** (3): 265-277.

609 21. M.J. Nueda, S. Tarazona, A. Conesa, *Bioinformatics*, 2014, **30** (18): 2598-2602.

610 22. M.J. Nueda, A. Conesa, J.A. Westerhuis, H.C.J. Hoefsloot, A.K. Smilde, M. Talón,
611 A. Ferrer, *Bioinformatics*, 2007, **23** (14): 1792-1800.

612 23. M.E. Smoot, K. Ono, J. Ruscheinski, P.L. Wang, T. Ideker, *Bioinformatics*, 2011,
613 **27** (3): 431–432.

614 24. M.J. Nueda, P. Sebastián, S. Tarazona, F. García-García, J. Dopazo, A. Ferrer, A.
615 Conesa, *BMC-Bioinfo*., 2009, **10** (6): S9.

616 25. F.C. Odds, A.J. Brown, N.A. Gow, *Trends Microbiol*., 2003 **11** (6): 272-279.

617 26. A.J. Carrillo-Muñoz, G. Giusiano, P.A. Ezkurra, G. Quindós, *Rev. Esp. Quimioter*.,
618 2006, **19** (2): 130-139.

619 27. J. Palma-Guerrero, H-B. Jansson, J. Salinas, L.V. Lopez-Llorca, *J. Appl. Microbiol*.,
620 2008, **104** (2): 541-553.

621 28. L.N. Nguyen, A. Gacser, J.D. Nosanchuk, *Virulence*, 2011, **2** (6): 538-541

622 29. Schauder, C.M., Wu, X., Saheki, Y., Narayanaswamy, P., Torta, F., Wenk,
623 M.R., De Camilli, P., and Reinisch, K.M. *Nature,* 2014, **510** (7506): 552-555.

624 30. A.K. Agarwal, P.D. Rogers, S.R. Baerson, M.R. Jacob, K.S. Barker, J.D. Cleary,
625 L.A. Walker, D.G. Nagle, A.M. Clark, *J. Biol. Chem*., 2003, **278** (37): 34998-5015.

626 31. C.F. Hoehamer, E.D. Cummings, G.M. Hilliard, P.D. Rogers, *Antimicrob. Agents.*
627 *Chemother*., 2010, **54** (5): 1655-1664.

628 32. E. Thomas, E. Roman, S. Claypool, N. Manzoor, J. Pla, S.L. Panwar, *Antimicrob.*
629 *Agents. Chemother*., 2013, **57** (11):5580-99

Published on 01 December 2015. Downloaded by Universidad de Alicante on 09/12/2015 15:48:54.

Molecular BioSystems Accepted Manuscript

View Article Online
DOI: 10.1039/C5MB00649J

Published on 01 December 2015. Downloaded by Universidad de Alicante on 09/12/2015 15:48:54.

630 33. H.L. Mobley, R.J. Doyle, U.N. Streips, S.O. Langemeier, *J. Bacteriol*., 1982, **150**
631 (1): 8-15.

632 34. B.M. Hayes, M.A. Anderson, A. Traven, N.L. van der Weerden, M.R. Bleackley,
633 *Cell. Mol. Life Sci.*, 2014, **71** (14): 2651-2666.

634 35. A. Castro, C. Lemos, A. Falcão, A.S. Fernandes, N.L. Glass, A. Videira, *Eukaryot.*
635 *Cell*., 2010, **9** (6): 906-914.

636 36. A.P. Gonçalves, C. Hall, D.J. Kowbel, N.L. Glass, A. Videira, *G3 (Bethesda)*,
637 2014, **4** (6): 1091-102.

638 37. F. Brodhun, I. Feussner, *FEBS J.*, 2011, **278** (7): 1047-1063.

639 38. A. Singh, M. Del Poeta, *Cell Microbiol*., 2011, **13** (2): 177-85.

640 39. Y. Yang, J.Z. Cheng, S.S. Singhal, M. Saini, U. Pandya, S. Awasthi, Y.C. Awasthi,
641 *J. Biol. Chem*., 2010, **276** (22): 19220-19230.

642 40. A.S. Fernandes, A. Castro, A. Videira, *Apoptosis*, 2013, **18** (8): 940-8.

643 41. L.S. Ryder, Y.F. Dagdas, T.A. Mentlak, M.J. Kershaw, C.R. Thornton, M. Schuster,
644 J. Chen, Z. Wang, N.J. Talbot, *Proc. Natl. Acad. Sci. USA*., 2013, **110** (8): 3179-
645 3184.

646 42. N. Cano-Domínguez, K. Álvarez-Delfín, W. Hansberg, J. Aguirre, *Eukaryot. Cell*.,
647 2008, **7** (8): 1352-1361.

648 43. Y. Yan, C.L. Wei, W.R. Zhang, H.P. Cheng, J. Liu, (2006) *Acta Pharmacol. Sin*.,
649 2006, **27** (7): 821-826.

650 44. A.P. Gonçalves, , J. Monteiro, , C. Lucchi, , D.J. Kowbel, , J.M. Cordeiro, , P.
651 Correia-de-Sá, , D.J. Rigden, N.L. Glass, A. Videira, *Microbial Cell.*, 2014, **1** (9):
652 289-302

653 45. P. D'hooge, C. Coun, V. Van Eyck, L. Faes, R. Ghillebert, L. Mariën, J.
654 Winderickx, G. Callewaert, *Cell Calcium*, 2015, **58** (2): 226-235.

Molecular BioSystems Accepted Manuscript

View Article Online
DOI: 10.1039/C5MB00649J

Published on 01 December 2015. Downloaded by Universidad de Alicante on 09/12/2015 15:48:54.

655 46. H.V. Colot, G. Park, G.E. Turner, C. Ringelberg, C.M. Crew, L. Litvinkova, RL
656 Weiss, K.A. Borkovich, J.C. Dunlap. *Proc. Natl. Acad. Sci. USA*., 2006, **103** (27):
657 10352-10357.

658 47. J.C. Dunlap, K.A. Borkovich, M.R. Henn, G.E. Turner, M.S. Sachs, N.L. Glass, K.
659 McCluskey, M. Plamann, J.E. Galagan, B.W. Birren, R.L. Weiss, J.P.
660 Townsend, J.J. Loros, M.A. Nelson, R. Lambreghts, H.V. Colot, G. Park, P.
661 Collopy, C. Ringelberg, C. Crew, L. Litvinkova, D. DeCaprio, H.M. Hood, S.
662 Curilla, M. Shi, M. Crawford, M. Koerhsen, P. Montgomery, L. Larson, M.
663 Pearson, T. Kasuga, C. Tian, M. Baştürkmen, L. Altamirano, J. Xu, *Adv. Genet*.,
664 2007, **57**:49-96.

665 48. K. McCluskey, *Adv. Appl. Microbiol*., 2003, **52**: 245-262.

666 49. C. Trapnell, L. Pachter, S.L. Salzberg, *Bioinformatics,* 2009, **25** (9):1105-1111.

667 50. B. Langmead, C. Trapnell, M. Pop, S.L. Salzberg, *Genome Biol.,* 2009, **10** (3):R25

668 51. A. Conesa, S. Götz, *Int. J. Plant Genomics*, 2008, 2008:619832.

669 52. R. Edgar, M. Domrachev, A.E. Lash, *Nucl. Ac. Res,* 2002, **30** (1):207-210.

670 53. R.D. Finn, J. Clements, S.R. Eddy, *Nucl. Ac. Res.*, 2011, **39**: 29-37.

671 54. P. Horton, K.J. Park, T. Obayashi, N. Fujita, H. Harada, C.J. Adams-Collier, K.
672 Nakai, *Nucleic. Acids. Res*., 2007, W585-587.

673 55. W. Gish, D.J. States, *Nature Genet*., 1993, (3): 266-272.

674 56. A. Conesa, M.J. Nueda, A. Ferrer, M. Talon, *Bioinformatics*, 2006, **22** (9): 1096-
675 1102**.**

676 57. S. Tarazona, S. Prado-López, J. Dopazo, A. Ferrer, A. Conesa, *Chemometr. Intell.*
677 *Lab. Syst*., 2012, **100**: 113-122.

678 58. K.J. Livak, T.D. Schmittgen, *Methods*, 2001, 25: 402-408.

679 59. H.E. Brockman, F.J. de Serres, *Genetics*, 1963, **48** (4): 597-604.

Molecular BioSystems Accepted Manuscript

View Article Online
DOI: 10.1039/C5MB00649J

680 60. A.C. Leeder, W. Jonkers, J. Li, N.L. Glass, *Genetics*, 2013, **195** (3): 883-898.

681 61. A. Subramanian, P. Tamayo, V.K. Mootha, S. Mukherjee, B.L. Ebert, M.A.
682 Gillette, A. Paulovich, S.L. Pomeroy, T.R. Golub, E.S. Lander, J.P. Mesirov, *Proc.*
683 *Natl. Acad. Sci. USA*, 2005, **102** (43): 15545–15550.

684 62. D. Merico, R. Isserlin, O. Stueker, A. Emili, G.D. Bader, *PLoS One*, 2010, **5** (11):
685 e13984.

686

687 # Figure legends

688 **Figure 1.** Time-course effect of chitosan on *N. crassa* conidia germination. **(A)**
689 *N. crassa* germination started prior to 4h then conidia develop a germ tube (6-8h) and
690 established a young mycelium before 16h. **(B)** Effect of chitosan on conidia germination
691 at 8h, IC_{50} (50% germination) was found at 0.5 µg ml^{-1} chitosan. IC_{50}: half maximal
692 inhibitory concentration.

693 **Figure 2**. Venn diagram of differential gene expression of *N. crassa* in response
694 to chitosan. **(A)** Complete differential gene expression (DGE) including induced and
695 repressed genes in the 4-16h time-course. **(B)** Increased DGE, up-regulated genes. **(C)**
696 Decreased DGE, down-regulated genes. **(D)** Fold-change of 22 genes significantly
697 differentially expressed in response to chitosan during the whole time-course
698 expermient.

699 **Figure 3.** Gene Ontology (GO) functional annotation of *N. crassa* genes
700 differentially expressed in response to chitosan. **(A)** Global GO annotation of
701 significantly expressed genes. **(B)** Selected GO-terms time-series with maSigFun
702 represented as the average expression profile of the associated genes to each GO.

703 **Figure 4. (A-D)** Time-series analysis of genes associated with the response of *N.*
704 *crassa* to chitosan by ASCA-genes. Graphs represent gene expression average trend of
705 four clusters of genes that follow the discovered general patterns of the ASCA model.
706 Genes that are well represented by the PC obtained with the ASCA model.

Published on 01 December 2015. Downloaded by Universidad de Alicante on 09/12/2015 15:48:54.

Molecular BioSystems Accepted Manuscript

View Article Online
DOI: 10.1039/C5MB00649J

Published on 01 December 2015. Downloaded by Universidad de Alicante on 09/12/2015 15:48:54.

Molecular BioSystems Accepted Manuscript

707 **Figure 5.** Effect of chitosan on growth of *N. crassa* WT and selected deletion
708 strains from RNAseq data. **(A)** Chitosan minimal inhibitory concentration (MIC) of
709 selected deletion strains and WT. **(B-E)** Fungal growth kinetics of **(B)** WT, **(C)**
710 ΔNCU03639, **(D)** ΔNCU04537 and **(E)** ΔNCU08770 in response to increasing
711 concentrations of chitosan (n=4; mean ± SE).

712 **Figure 6.** Effect of Ca^{2+} on chitosan antifungal activity to *N. crassa* WT and
713 deletion strains from membrane remodeling genes (ΔNCU10610 and ΔNCU03263-Δ
714 *syt 1*). (A) *N. crassa* WT growth in response to chitosan (0.5 µg ml-1) under several
715 Ca^{2+} concentrations. (B) Nuclear damage after treatment of conidia of a strain in which
716 PI has been targeted to the nuclei. Conidia treated with chitosan and stained with 2 µg
717 ml^{-1} propidium iodide (PI). Fluorescence images right and DIC images of same conidia
718 on the left. Bar = 5 µm. (C) Evaluation of conidia viability treated with chitosan and
719 Ca^{2+} stained with PI.

720 **Figure 7.** Cytoscape network of functional gene annotation of *N. crassa* gene
721 response to chitosan. Large font tittles represents a summary of GO-terms found
722 enriched in clusters. Node size correlates to the number of genes annotated to that
723 functional category. Each node represents a gene function significantly enriched (FDR≤
724 0.1).

725 **Figure 8.** Key genes associated with *N. crassa* response to chitosan. In this
726 model, NCU03639 would increase membrane permeability by altering mechanisms of
727 plasma membrane remodeling and fluidity. NCU10610 (Ca^{2+} regulator with *fig 1*
728 domain) would be associated with the mechanisms of plasma membrane remodeling
729 mediated by Ca^{2+}. NCU04534 (MFS transporter) could be involved in mechanisms of
730 assimilation or detoxification monosaccharaides (e.g. monomers of N-acetyl
731 glucosamine). NCU10521 (glutathione transferase), NCU01849 and NCU01071
732 (dioxygenases) would be related with the response of the fungus to the oxidative stress,
733 the key response of *N. crassa* to chitosan. Genes involved in mechanisms associated
734 with protein synthesis (NCU04555) and resistance to chemical compounds
735 (NCU02363) are also differentially expressed in response to chitosan.

736

View Article Online
DOI: 10.1039/C5MB00649J

737

738

739

740

741

742

Published on 01 December 2015. Downloaded by Universidad de Alicante on 09/12/2015 15:48:54.

Molecular BioSystems Accepted Manuscript

View Article Online
DOI: 10.1039/C5MB00649J

Published on 01 December 2015. Downloaded by Universidad de Alicante on 09/12/2015 15:48:54.

Fig. 1

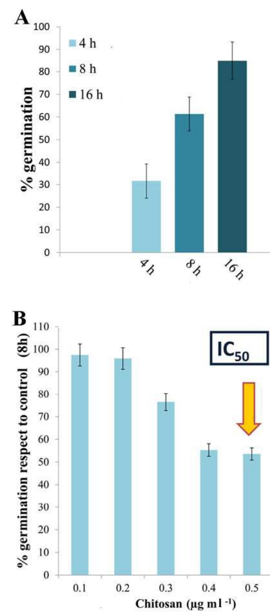

209x270mm (254 x 254 DPI)

Molecular BioSystems Accepted Manuscript

View Article Online
DOI: 10.1039/C5MB00649J

Published on 01 December 2015. Downloaded by Universidad de Alicante on 09/12/2015 15:48:54.

Fig. 2

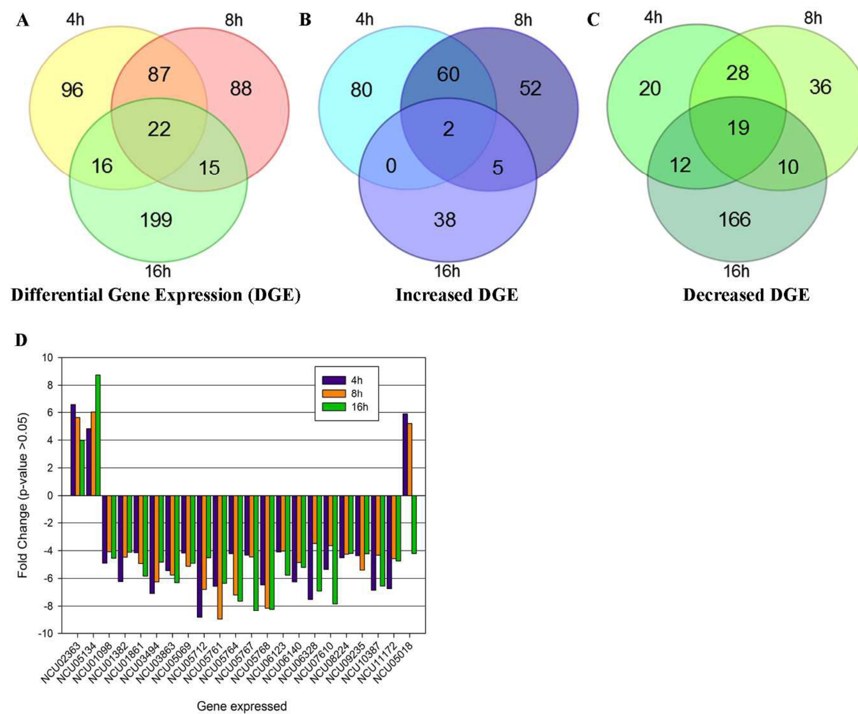

209x270mm (254 x 254 DPI)

Molecular BioSystems Accepted Manuscript

View Article Online
DOI: 10.1039/C5MB00649J

Published on 01 December 2015. Downloaded by Universidad de Alicante on 09/12/2015 15:48:54.

Fig. 3

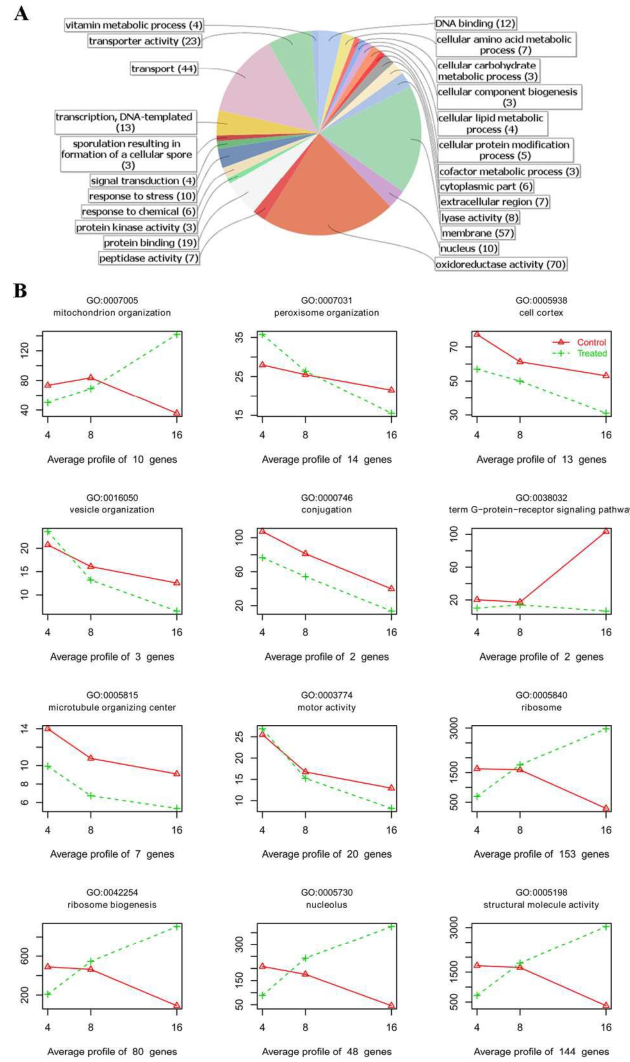

209x270mm (254 x 254 DPI)

Molecular BioSystems Accepted Manuscript

View Article Online
DOI: 10.1039/C5MB00649J

Published on 01 December 2015. Downloaded by Universidad de Alicante on 09/12/2015 15:48:54.

Fig. 4

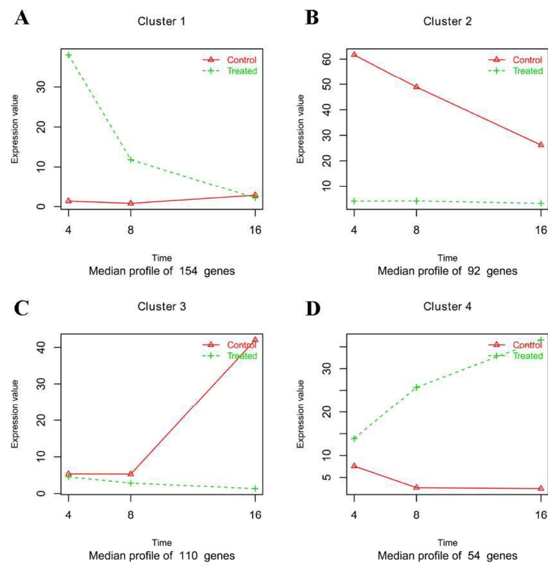

209x270mm (254 x 254 DPI)

Molecular BioSystems Accepted Manuscript

View Article Online
DOI: 10.1039/C5MB00649J

Published on 01 December 2015. Downloaded by Universidad de Alicante on 09/12/2015 15:48:54.

Fig. 5

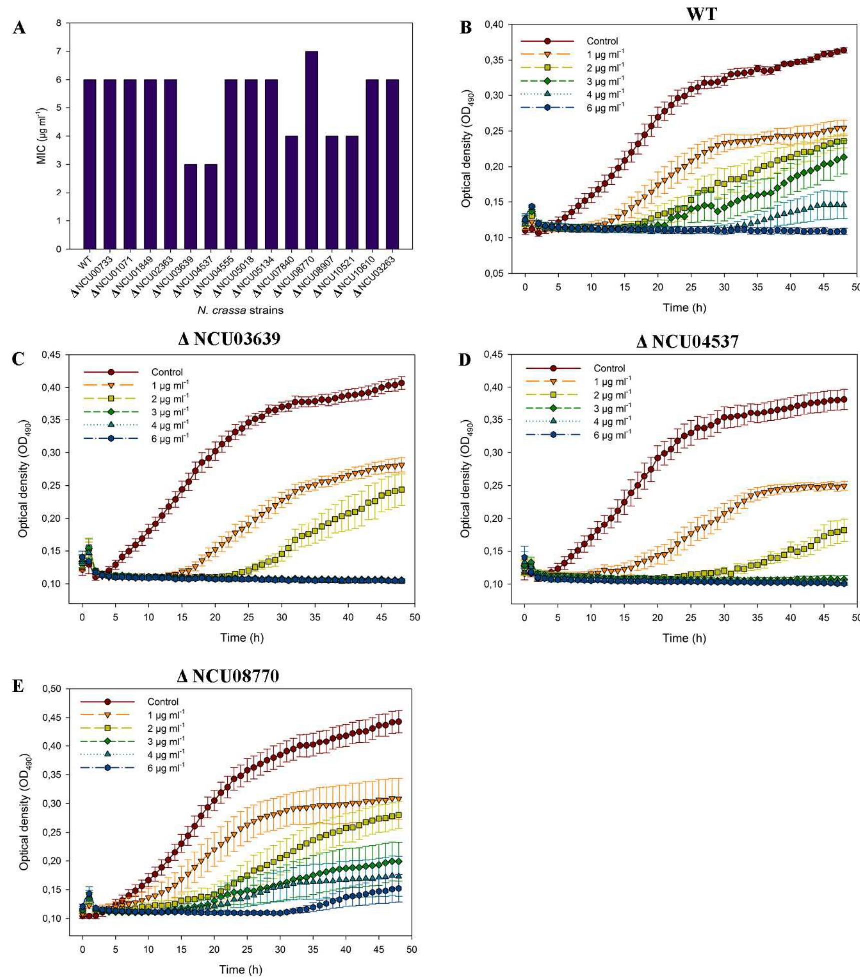

209x270mm (254 x 254 DPI)

Molecular BioSystems Accepted Manuscript

View Article Online
DOI: 10.1039/C5MB00649J

Published on 01 December 2015. Downloaded by Universidad de Alicante on 09/12/2015 15:48:54.

Fig. 6

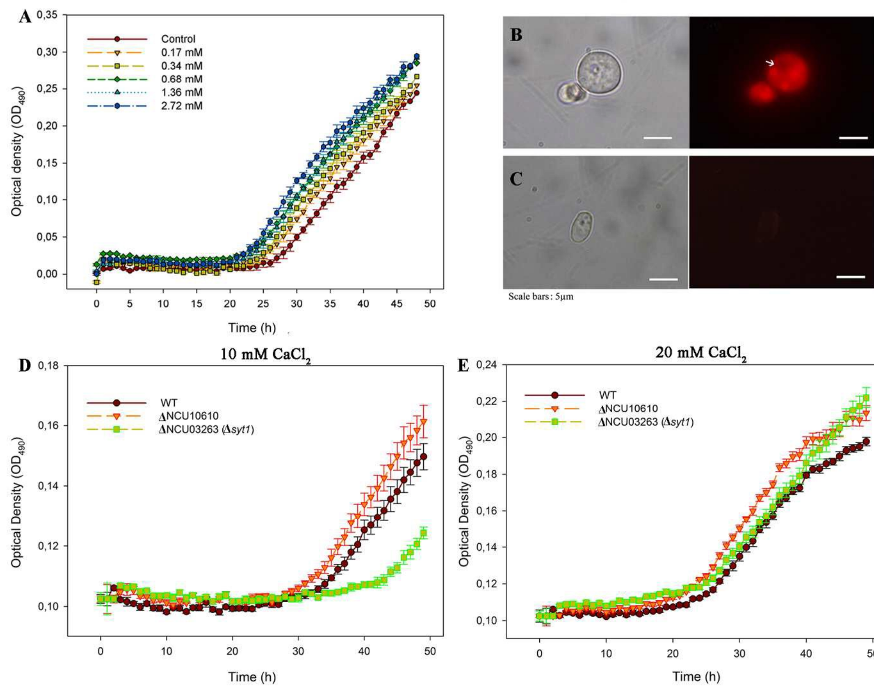

209x270mm (254 x 254 DPI)

Molecular BioSystems Accepted Manuscript

View Article Online
DOI: 10.1039/C5MB00649J

Fig. 7

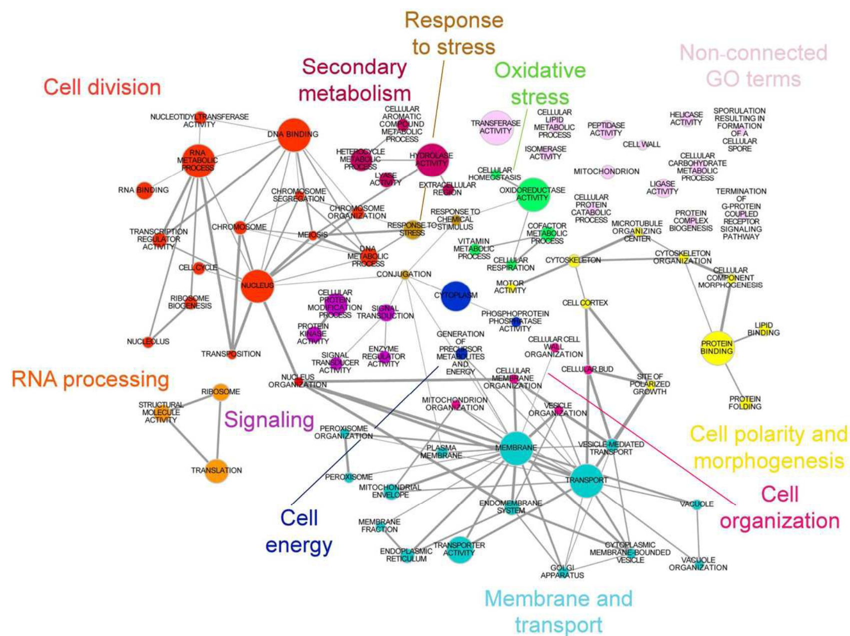

209x270mm (254 x 254 DPI)

Published on 01 December 2015. Downloaded by Universidad de Alicante on 09/12/2015 15:48:54.

Molecular BioSystems Accepted Manuscript

View Article Online
DOI: 10.1039/C5MB00649J

Published on 01 December 2015. Downloaded by Universidad de Alicante on 09/12/2015 15:48:54.

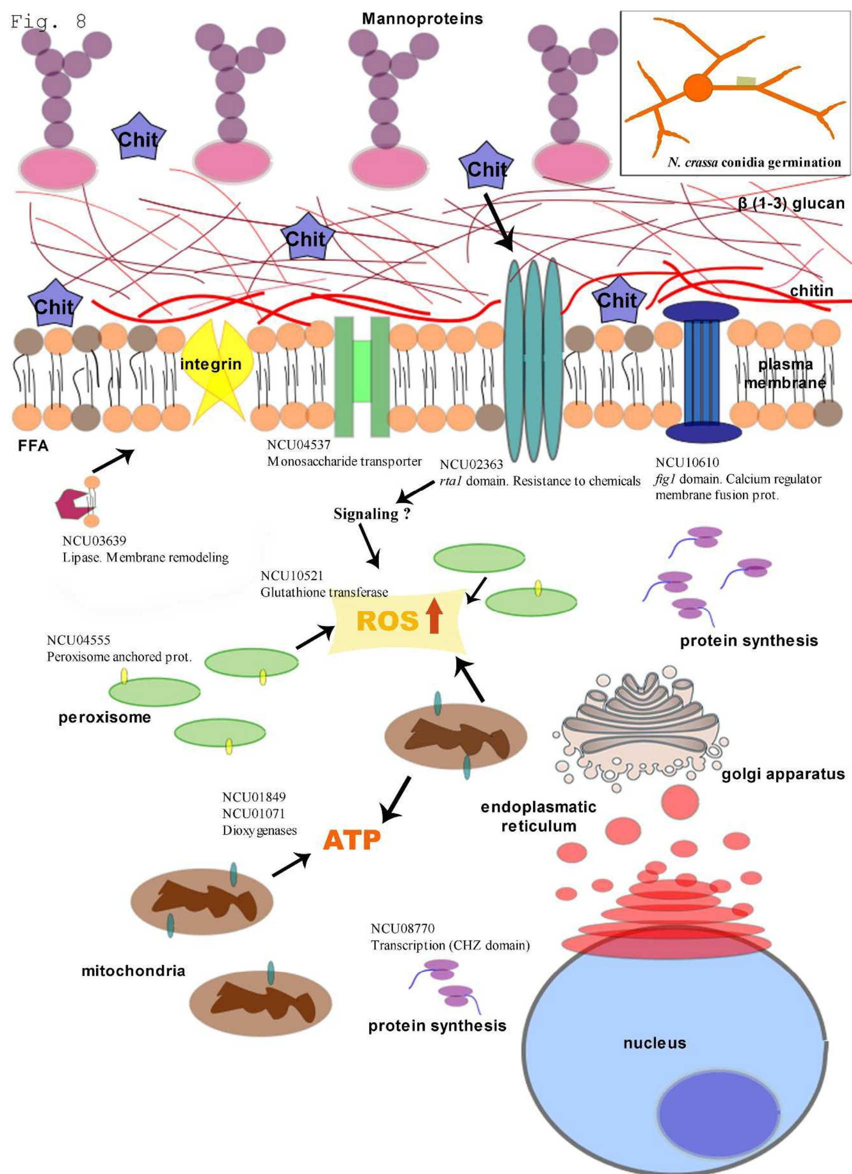

371x525mm (300 x 300 DPI)

Molecular BioSystems Accepted Manuscript